Published in final edited form as:
Biochemistry. 2003 December 2; 42(47): 13929–13940. doi:10.1021/bi034843p.

Pancreatic Islets and Insulinoma Cells Express a Novel Isoform of Group VIA Phospholipase A_2 (iPLA$_2$β) that Participates in Glucose-Stimulated Insulin Secretion and Is Not Produced by Alternate Splicing of the iPLA$_2$β Transcript†

Sasanka Ramanadham[*,‡], **Haowei Song**[‡], **Fong-Fu Hsu**[‡], **Sheng Zhang**[‡], **Mark Crankshaw**[§], **Gregory A. Grant**[§], **Christopher B. Newgard**[‖], **Shunzhong Bao**[§], **Zhongmin Ma**[⊥], and **John Turk**[‡]

Mass Spectrometry Resource, Division of Endocrinology, Diabetes, and Metabolism, Department of Medicine, and Protein and Nucleic Acid Chemistry Laboratory, Washington University School of Medicine, St. Louis, Missouri 63110, Sarah W. Stedman Center for Nutritional Studies, Department of Pharmacology and Cancer Biology, Duke University Medical Center, Durham, North Carolina 27710, and Mount Sinai School of Medicine, New York, New York 10029

Abstract

Many cells express a group VIA 84 kDa phospholipase A_2 (iPLA$_2$β) that is sensitive to inhibition by a bromoenol lactone (BEL) suicide substrate. Inhibition of iPLA$_2$β in pancreatic islets and insulinoma cells suppresses, and overexpression of iPLA$_2$β in INS-1 insulinoma cells amplifies, glucose-stimulated insulin secretion, suggesting that iPLA$_2$β participates in secretion. Western blotting analyses reveal that glucose-responsive 832/13 INS-1 cells express essentially no 84 kDa iPLA$_2$β-immunoreactive protein but predominantly express a previously unrecognized immunoreactive iPLA$_2$β protein in the 70 kDa region that is not generated by a mechanism of alternate splicing of the iPLA$_2$β transcript. To determine if the 70 kDa-immunoreactive protein is a short isoform of iPLA$_2$β, protein from the 70 kDa region was digested with trypsin and analyzed by mass spectrometry. Such analyses reveal several peptides with masses and amino acid sequences that exactly match iPLA$_2$β tryptic peptides. Peptide sequences identified in the 70 kDa tryptic digest include iPLA$_2$β residues 7–53, suggesting that the N-terminus is preserved. We also report here that the 832/13 INS-1 cells express iPLA$_2$β catalytic activity and that BEL inhibits secretagogue-stimulated insulin secretion from these cells but not the incorporation of arachidonic acid into membrane PC pools of these cells. These observations suggest that the catalytic iPLA$_2$β

†This research was supported in part by grants from National Institutes of Health (R37-DK34388, P41-RR00954, P01-HL57278, P60-DK20579, P30-DK56341) and by an Award (S.R.) from the American Diabetes Association.

[*]Corresponding author. Tel: (314) 362-8194. Fax: (314) 362-8188. sramanad@im.wustl.edu..
[‡]Division of Endocrinology, Diabetes, and Metabolism, Washington University School of Medicine.
[§]Protein and Nucleic Acid Chemistry Laboratory, Washington University School of Medicine.
[‖]Duke University Medical Center.
[⊥]Mount Sinai School of Medicine.

[1]Abbreviations: AA, arachidonic acid; BEL, bromoenol lactone suicide inhibitor of iPLA$_2$β; BME, β-mercaptoethanol; BSA, bovine serum albumin; bp, base pairs; cPLA$_2$, Group IV cytosolic phospholipase A_2; dpm, disintegrations per minute; ECL, enhanced chemiluminescence; FBS, fetal bovine serum; GPC, glycerophosphocholine; IF, immunofluorescence; iPLA$_2$β, β-isoform of Group VIA calcium-independent phospholipase A_2; kDa, kilodaltons; LC/ESI, liquid chromatography/electrospray ionization; MALDI/TOF, matrix-assisted laser desorption ionization/time-of-flight; MS, mass spectrometry; OE, iPLA$_2$β overexpressing cells; O/N, overnight; PAGE, polyacrylamide gel electrophoresis; Q-TOF, quadrupole-time-of-flight; PBS, phosphate-buffered saline; PC, phosphatidylcholine; piPLA$_2$, polyclonal iPLA$_2$; PIC, protease inhibitor cocktail; PLA$_2$, phospholipase A_2; SDS, sodium dodecyl sulfate; TBS-T, Tris-buffered saline-tween; TLC, thin-layer chromatography; RT, room temperature; RT-PCR, reverse transcription-polymerase chain reactions; V, empty vector transfected cells.

activity expressed in 832/13 INS-1 cells is attributable to a short isoform of iPLA$_2$β and that this isoform participates in insulin secretory but not in membrane phospholipid remodeling pathways. Further, the finding that pancreatic islets also express predominantly a 70 kDa iPLA$_2$β-immunoreactive protein suggests that a signal transduction role of iPLA$_2$β in the native β-cell might be attributable to a 70 kDa isoform of iPLA$_2$β.

Phospholipases A$_2$ (PLA$_2$)[1] are a diverse group of enzymes that catalyze hydrolysis of the *sn*-2 substituent from glycerophospholipid substrates to yield a free fatty acid and a 2-lyso-phospholipid (1). At present, the recognized PLA$_2$s are classified into 14 groups (2), and among the PLA$_2$s is an 84 kDa cytosolic PLA$_2$ that does not require Ca^{2+} for catalysis and is classified as group VIA PLA$_2$. This enzyme designated iPLA$_2$β (3–5) is activated by ATP and inhibited by a bromoenol lactone (BEL) suicide substrate (6, 7). Inhibition of iPLA$_2$β with BEL or antisense oligonucleotide has been reported to suppress the incorporation of arachidonic acid into membrane phospholipids of macrophage-like P388D1 cells (8, 9) leading to the suggestion that iPLA$_2$β participates in phospholipid remodeling (10, 11). Findings in other cells, however, suggest that iPLA$_2$β is involved in signal transduction (12–18).

The iPLA$_2$ has been cloned from several sources and is encoded by mRNA species that yield a protein with an expected molecular mass of 84–88 kDa and contains a lipase motif preceded by eight N-terminal ankyrin repeats (7, 19, 20). The 88 kDa iPLA$_2$β isoform is a product of a mRNA species that arises from an exon-skipping mechanism of alternate splicing (21) and contains a 54 amino acid sequence that interrupts the eighth ankyrin repeat. At least three additional human iPLA$_2$β transcripts exhibiting distinct tissue distribution and cellular localization have also been reported (22). These transcripts, also generated via alternate splicing, encode shorter iPLA$_2$β protein sequences that terminate after the lipase active site and after the ankyrin-repeat sequence (21). Interestingly, whereas the transfection of COS cells with full-length iPLA$_2$β cDNA is reflected by a significant increase in iPLA$_2$β enzymatic activity, transfection with cDNA encoding the shorter protein does not increase enzymatic activity above the background. Further, cotransfection of the two cDNAs results in a reduction in enzymatic activity, suggesting that protein products of alternate spliced transcripts can function as negative modulators of iPLA$_2$β activity.

Recent reports suggest that the full-length iPLA$_2$β protein is also a candidate for proteolytic cleavage (23, 24). In contrast to products generated by the alternate splicing of the iPLA$_2$β transcript, proteolytic processing of the iPLA$_2$β protein appears to yield truncated products that are constitutively active. Examples include a caspase-3-catalyzed N-terminal cleavage of iPLA$_2$β in human promonocytic U937 cell (23) and a calmodulin-dependent C-terminal cleavage of iPLA$_2$β under in vitro conditions (24).

Here, we report that 832/13 INS-1 cells, which secrete insulin robustly in response to glucose, parental INS-1 cells, and pancreatic islets, express predominantly a iPLA$_2$β-immunoreactive species that migrates with an apparent molecular mass of 70 kDa on SDS–PAGE analyses. As essentially no 84–88 kDa iPLA$_2$β-immunoreactive protein is observed in these preparations, we used mass spectrometric analyses to examine whether the 70 kDa-immunoreactive material is in fact a iPLA$_2$β isoform.

MATERIALS AND METHODS

Materials

INS-1 cells were generously provided by Dr. C. Newgard (Duke University Medical Center, Durham, NC). Other materials were obtained from the following (sources):

[5,6,8,9,11,12,14,15-^{3}H]-arachidonic acid (217 Ci/mmol), enhanced chemiluminescence (ECL) reagent, and (16:0/[^{14}C]-18:2)-GPC (PLPC, 55 mCi/mmol) (Amersham Biosciences, Piscataway, NJ); standard phospholipids (Avanti Polar Lipids, Birmingham, AL); sodium dodecyl sulfate–polyacrylamide gel electrophoresis (SDS–PAGE) supplies and Sypro Ruby protein stain (BioRad, Richmond, CA); organic solvents (Fisher Scientific, Pittsburgh, PA); agarose, kb standards, and RT-PCR reagents (Invitrogen, Carlsbad, CA); normal goat serum and Cy3-conjugated affinipure goat anti-rabbit IgG (H+L) (Jackson Immuno Research Laboratories, West Grove, PA); HPLC columns and precolumns (LC Packings, San Francisco, CA); pentex fraction V fatty acid-free bovine serum albumin (ICN Biomedicals Inc., Aurora, OH); Coomasie reagent (Pierce, Rockford, IL); peroxidase-conjugated goat anti-rabbit IgG antibody (Roche Diagnostic Corporation, Indianapolis, IN); ATP-agarose column, α-cyano 4-hydroxy cinnamic acid, arachidonic acid, forskolin, fraction V bovine albumin, globulin-free bovine albumin, protease inhibitor cocktail (PIC), common reagents and salts, and protein standards for MS (Sigma Chemical Co., St. Louis, MO); and antibiotic solutions and cell culture media (Tissue Culture Support Center, Washington University, St. Louis, MO).

Cell Culture

A retroviral system (25) was used to stably transfect INS-1 cells with either an empty retroviral (V) construct or with a construct containing iPLA$_2$β cDNA as an insert (OE) to achieve overexpression, as described (7). The V, OE, and 832/13 INS-1 cells were cultured, as described (26, 27), at 37 °C in a humidified atmosphere containing 5% CO_2.

Western Blotting Analyses of iPLA$_2$β Protein

INS-1 cell and pancreatic islet cytosolic protein were analyzed by SDS–PAGE (7.5%), transferred onto Immobolin-P PVDF membranes, and processed for immunoblotting analyses, and iPLA$_2$β-immunoreactive protein bands were visualized by ECL, as described (28).

iPLA$_2$ Message Expression in INS-1 Cells

Polymerase chain reactions (PCR) were performed, as described (29), using primer pair (sense, 5′-CAGAGAATGAGGAGGGCTGT-3′ and antisense, 5′-CCGACCATCTCACACCAGGC-3′, expected product size 1660 base pairs) for iPLA$_2$β, based on the rat sequence (7). Restriction enzyme analyses were then performed to confirm that the PCR products are amplified from the iPLA$_2$β mRNA. Reaction mixtures were analyzed by 1% agarose gel electrophoresis, and reaction products were visualized by ethidium bromide staining.

To examine if the 832/13 INS-1 cells express an alternatively spliced message for iPLA$_2$β that encodes a 70 kDa iPLA$_2$β isoform, PCR analyses were performed using overlapping primer sets covering the entire length (2259 bases) of the iPLA$_2$β message (7) encoding an 84 kDa iPLA$_2$β protein. The five sense/antisense primer sets and the iPLA$_2$β message region covered with each set were (1) ATGCAGTTCTTGGACGCCTCGT/ AGTACTGTACCAACTCCA, 1–523; (2) CGCCAACAGCACAGAGAA/ CATAGGTCAGCAGCACCA, 429–1017; (3) TGACGTGGACAGCACAAG/ AGACTCATAGGGCCGTGA, 924–1509; (4) TACACAGTAAATCCATGG/ CCAGTTCCTTGGCTCCAA, 1424–2020; and (5) GGAAAGTCCCCTCAAGTG/ TCAGGGAGATAGCAGCAGCT, 1924–2259). Reaction products were then purified for sequence analyses.

Mass Spectrometric Analyses of Protein in the 70 kDa Region. Sample Preparation

To determine whether the iPLA$_2$β-immunoreactive band in the 70 kDa region of the SDS–PAGE gels represented a iPLA$_2$β isoform, INS-1 cells (1.4×10^9) were homogenized (10 mM HEPES, 1 mM EDTA, 340 mM sucrose, 1 mM DTT, pH 7.5) and sonicated (Sonics & Materials Vibra Cell, 12%, 10 s), and the pooled sonicate was centrifuged (1000*g*, 10 min, 4 °C). Protein in the supernatant was precipitated overnight with ammonium sulfate (50%), and the mixture was centrifuged (20 000*g*, 30 min). The resultant protein pellet was resuspended in buffer A (10 mM HEPES, 1 mM EDTA, 340 mM sucrose, 1 mM DTT, 1 mM Triton X-100, pH 7.5) and loaded onto an ATP-agarose affinity column (1.5 mL). iPLA$_2$β was eluted from the column as previously described (30), and fractions containing activity were concentrated and analyzed by SDS–PAGE (7.5%). After identification of the iPLA$_2$β-immunoreactive bands, the corresponding regions were excised from a Ruby-stained gel and digested with trypsin (0.15 μg, O/N at 37 °C) prior to analyses by MS analyses.

MALDI/TOF/MS Analyses

Tryptic digest was mixed (1:1, v/v) with saturated α-cyano-4-hydroxycinnamic acid matrix solution (1 mg of matrix in 100 μL of dH_2O), and an aliquot (1 μL) of the sample mixture was spotted on a MALDI plate. The mass spectrometer was calibrated with a mixture of leucine-enkephalin, bradykinin, glu-fibrino-peptide B, and bovine insulin. Internal calibration of samples was achieved using typsin-autodigestion peptides with $[M + H]^+$ ion *m*/*z* values of 842.5100 and 2211.1892. MALDI mass spectra were acquired on an Applied Biosystems Voyager-DE STR with a delayed extraction in reflectron mode.

LC/ESI/MS/MS Analyses

An aliquot (0.05 μL) of tryptic digest was injected into a Micromass CapLC system (Micromass, Manchester, UK) and preconcentrated on a 300 μm × 5 mm PepMap C18 precolumn. For chromatographic separation, a gradient was generated over 50 min at a flow rate of 200 nL/min of solution A (3% acetonitrile/97% water) and solution B (95% acetonitrile/5% water), both containing 0.1% formic acid. The LC eluent from this column was directly introduced to the nanoflow source of a Micromass QTOF micromass spectrometer (Manchester, UK). The instrument was calibrated with a multi-point calibration using selected fragment ions that resulted from collision-induced decomposition of standard glu-fibrino-peptide B. The data were analyzed using Mascot Search and MassLynx V3.5 softwares.

iPLA$_2$β Enzymatic Activity Assay

Ca^{2+}-independent PLA$_2$ enzymatic activity in cytosolic and membrane fractions (30 μg of protein) in the absence and presence of ATP (10 mM) or BEL (10 μM) was assayed by ethanolic injection (5 μL) of the substrate 1-palmitoyl-2-[^{14}C]linoleoyl-*sn*-glycero-3-phosphocholine (5 μM) in assay buffer (40 mM Tris, pH 7.5, 5 mM EGTA), as previously described (6).

Incubation of 832/13 INS-1 Cells with Arachidonic Acid to Induce Phospholipid Remodeling and Mass Spectrometric Characterization of Phospholipids

832/13 INS-1 cells (1×10^6/condition) were treated (30 min, 37 °C) with vehicle or with BEL (25 μM), as described (5, 31). The culture medium was then removed and replaced with fresh medium supplemented with arachidonic acid (final concentration, 70 μM), and the cells were cultured (37 °C) for 24 h. At various times, lipids were extracted and analyzed by NP-HPLC to isolate glycerophosphocholine (GPC) lipids, which were analyzed as Li^+ adducts by ESI/MS/MS in a positive ion mode, as described (5, 31, 32).

Insulin Secretion by 832/13 INS-1 Cells

832/13 INS-1 cells seeded in 24-well plates were incubated (1 h, 37 °C, 95% air/5% CO_2) with Krebs–Ringer buffer [KRB, pH 7.3, containing (in mM): NaCl (115), $NaHCO_3$ (24), KCl (5), $MgCl_2$ (1), Hepes (25), glucose (1), and 0.10% BSA] containing glucose (0–20 mM) without or with IBMX (100 μM) or forskolin (FSK, 2.5 μM), as described (30). Effects of BEL on stimulated secretion were examined by including BEL (10 μM in KRB media without BSA) during the preincubation period. At the end of the incubation period, medium was removed for the measurement of insulin by radioimmunoassay.

RESULTS

Immunoblotting Analyses Suggest Expression of a Short iPLA$_2$β Isoform in INS-1 Cells

To determine if 832/13 INS-1 cells express iPLA$_2$β protein, cytosolic protein prepared from these cells and from stably transfected INS-1 cells overexpressing iPLA$_2$β (OE) or empty vector (V) alone was processed for Western blotting analyses. As expected, an intense band in the 84 kDa region is evident in the OE cells (Figure 1), reflecting the expression of the full-length iPLA$_2$β protein, as previously reported (7). In addition, a second iPLA$_2$β-immunoreactive band with an apparent molecular mass of ca. 70 kDa is also observed. In contrast, the V and 832/13 INS-1 cells do not express full-length iPLA$_2$β at levels comparable to the OE cell line. Both V and 832/13 INS-1 cells, however, do express a iPLA$_2$β-immunoreactive band in the 70 kDa region that could represent a previously unrecognized short form of iPLA$_2$β.

832/13 INS-1 Cells Express mRNA Encoding iPLA$_2$β

We next determined if the 832/13 INS-1 cells express message for iPLA$_2$β. Total RNA from the 832/13, V, and OE INS-1 cells was used as a template in RT-PCR analyses. As illustrated in Figure 2, a single PCR product of the size expected (1660 bp) from the iPLA$_2$β primer pair used was generated using cDNA from each of the three cell lines as a template, indicating that all three lines express message for iPLA$_2$β.

To verify that the RT-PCR fragments were amplified from iPLA$_2$β mRNA, the PCR products were digested with restriction enzymes *BamH I* or *Nco I*. The expected product fragment sizes with *BamH I* are 406 and 1254 bp and with *Nco I* are 996 and 664 bp. As seen in Figure 2, the restriction enzyme fragments from the PCR products are of the expected sizes, confirming that the 832/13 INS-1 cells express message for iPLA$_2$β.

To examine if the 832/13 INS-1 cells express an alternate spliced transcript that encodes a shorter iPLA$_2$β, five sets of overlapping iPLA$_2$β-specific primers designed to amplify the entire iPLA$_2$β encoding region (Figure 3A) were used to perform PCR analyses (Figure 3B). The PCR products (1–5, 4a, and 5a) from each reaction were then purified and sequenced. The sequences of PCR products 1–5 were found to match exactly with the predicted sequences and sizes illustrated in Figure 3A and encompass the complete iPLA$_2$β message sequence that encodes for the full-length iPLA$_2$β protein. The PCR products 4a and 5a were cloned into pGEM and sequenced, and neither sequence was found to have homology with any region of the iPLA$_2$β message. These findings reveal that the 832/13 INS-1 cells express a single iPLA$_2$β transcript that encodes a full-length 84 kDa iPLA$_2$β protein, suggesting that the expression of a 70 kDa iPLA$_2$β-immunoreactive protein is not a result of an exon-skipping mechanism of alternate splicing.

Mass Spectrometric Analyses Demonstrate a 70 kDa iPLA$_2$β Isoform

Mass spectrometric analyses were next used to obtain sequence information to establish the identity of the 70 kDa immunoreactive band. The INS-1 cell cytosol was subjected to ATP-

agarose affinity chromatography, the eluted fractions containing iPLA$_2$β activity were concentrated and analyzed by SDS–PAGE, and the resolved proteins were visualized with Ruby staining. Tryptic digests of protein bands in the 84 and 70 kDa-immunoreactive regions were then prepared separately and analyzed by MALDI/TOF/MS and peptide mass mapping followed by LC/ESI/MS/MS to determine the amino acid sequence of selected peptides. Such MS analyses of the 84 kDa iPLA$_2$β-immunoreactive protein identified several peptides from the iPLA$_2$β deduced amino acid sequence (data not shown).

Analyses of the tryptic digest of 70 kDa-immunoreactive material by MALDI/TOF/MS also reveal 10 peptides with *m*/*z* values expected of tryptic peptides from the iPLA$_2$β protein (Figure 4). Analyses of the tandem spectra obtained from LC/ESI/MS/MS in the tryptic digest prepared from the 70 kDa iPLA$_2$β-immunoreactive protein reveal several peptides with amino acid sequences that matched tryptic fragments from the iPLA$_2$β protein (Table 1). Figure 5 illustrates the tandem spectrum of one such peptide. The figure illustrates the observed *y*- and *b*-series ions arising from a peptide with an observed $[M + 2H]^{2+}$ *m*/*z* of 955.0425 (calculated M_r = 1908.0773). Analyses of the tandem spectrum with MassLynx Software identify the peptide sequence LVNTLSSVTNLFSNPFR as the most likely (99.89%) to exhibit the observed peptide fragmentation pattern. The sequence LVNTLSSVTNLFSNPFR exactly matches the expected tryptic peptide residues 7–23 from iPLA$_2$β. Of the expected product ions, nearly all of the predicted *y*- and *b*-series ions are represented in the tandem spectrum.

Similar tandem MS analyses identified nine additional iPLA$_2$β-tryptic peptides in the digest of the 70 kDa region of the gel (Table 1). The peptide sequences identified represent 17% coverage of the full-length 84 kDa iPLA$_2$β sequence. As illustrated in Table 1, the N-terminal region is prominently represented by fragments 6, 9, and 10, which include coverage of iPLA$_2$β amino acid sequence 7–53. The furthest identified region of coverage includes amino acid residue 555 (fragment 2). Thus, the MS analyses of the 70 kDa iPLA$_2$β-immunoreactive protein identify it as a short iPLA$_2$β isoform.

Expression of Ca^{2+}-Independent PLA_2 Enzymatic Activity by 832/13 INS-1 Cells

We next examined if the 832/13 INS-1 cells express Ca^{2+}-independent PLA_2 enzymatic activity. As illustrated in Figure 6, these cells express a cytosolic and membrane-associated Ca^{2+}-independent PLA_2 enzymatic activity. To verify that this activity is attributable to iPLA$_2$β, the ability of ATP to stimulate and of BEL to inhibit the enzymatic activity, as in pancreatic islets (6, 31, 33), was determined. The Ca^{2+}-independent PLA_2 enzymatic activity expressed in the 832/13 INS-1 cells is stimulated 3-fold by ATP and completely inhibited by BEL. These findings confirm that the 832/13 INS-1 cells express a iPLA$_2$β catalytic activity and suggest that it is most likely attributable to a 70 kDa isoform of iPLA$_2$β.

Inhibition of iPLA$_2$β Activity with BEL Does Not Affect Arachidonic Acid Incorporation into 832/13 INS-1 Cell Phosphatidylcholine

We next examined the role of a 70 kDa isoform of iPLA$_2$β in the 832/13 INS-1 cells. In P338D1 macrophage-like cells, the inhibition of iPLA$_2$β activity with BEL suppressed incorporation of arachidonic acid into phosphatidylcholine (PC) (8), leading to the suggestion that iPLA$_2$β is involved in membrane phospholipid remodeling. Similar analyses were performed in the present study to examine if iPLA$_2$β participates in phospholipid remodeling in the 832/13 INS-1 cells.

The ESI/MS spectra of Li^+ adducts of 832/13 INS-1 cell PC species are illustrated in Figure 7. Major ions in the spectrum of vehicle-treated cells (Figure 7A) represent Li^+ adducts of

16:0/16:1-GPC (*m*/*z* 738), 16:1/18:1-GPC (*m*/*z* 764), 16:0/18:1-GPC (*m*/*z* 766), and 18:1/18:1-GPC (*m*/*z* 792). The identities of the species represented by these ions were determined by collisionally-activated dissociation (CAD) and tandem MS (32).

In the tandem spectra of Li^+ adducts of GPC lipids, the identity of the headgroup is established by ions reflecting the loss of phosphocholine with lithium ($[M + Li – 189]^+$) or with hydrogen ($[M + Li – 183]^+$) (32), and ions reflecting these two losses are present in the spectrum (Figure 8A). The identities of fatty acid substituents in the GPC–Li^+ species are reflected by ions representing the loss of trimethylamine plus either the *sn*-1 or the *sn*-2 substituent as a free fatty acid, and the relative abundance of the former ion exceeds that of the latter, allowing positional assignments. The CAD of the $[M + Li]^+$ ion at *m*/*z* 788 (Figure 8A) from the 832/13 INS-1 cells yields a spectrum that contains an ion at *m*/*z* 473 (loss of trimethylamine plus palmitic acid) and a less abundant ion at *m*/*z* 425 (loss of trimethylamine plus arachidonic acid), thereby establishing the identity of the parent ion as 16:0/20:4-GPC-Li^+. Ions reflecting the loss of arachidonic acid (*m*/*z* 484), of palmitic acid (*m*/*z* 532), and of the lithium salts of these fatty acids (*m*/*z* 478 and 526, respectively) are also observed in the spectrum, as is an ion reflecting the loss of trimethylamine alone (*m*/*z* 729).

Figure 8B illustrates the ions expected from the fragmentation of 16:0/20:4-GPC-Li^+. All of these expected fragment ions are represented in the CAD spectrum of the $[M + Li]^+$ adduct ion at *m*/*z* 788 (Figure 8A).

Similar features of other tandem spectra identify arachidonate-containing species at *m*/*z* 788 (16:0/20:4-GPC), *m*/*z* 814 (18:1/20:4-GPC), and *m*/*z* 816 (18:0/20:4-GPC) in the untreated 832/13 INS-1 cells (Figure 7A). Addition of arachidonic acid to the culture medium induces the 832/13 INS-1 cells to remodel their phospholipids, as reflected by time-dependent increases in the abundances of arachidonate-containing PC species. After 6 h, signals for 16:0/20:4-GPC, 18:1/20:4-GPC, and 18:0/20:4-GPC increase several-fold (Figure 7B), and by 24 h 16:0/20:4-GPC and 18:0/20:4-GPC become two of the most abundant PC species in the mixture (Figure 7C). The increases in arachidonate-containing PC species at 24 h are unaffected by the pretreatment of 832/13 INS-1 cells with BEL, at concentrations that inhibit $iPLA_2\beta$ enzymatic activity for the duration of the experiment (Figure 7D). These findings do not support a role for $iPLA_2\beta$ in arachidonic acid incorporation into 832/13 INS-1 cell PC.

Stimulated Insulin Secretion from 832/13 INS-1 Cells Is Inhibited by BEL

A second proposed role for $iPLA_2\beta$ involves its participation in signal transduction (6, 7, 12–18, 33–36). The 832/13 INS-1 cell line has been demonstrated to exhibit a glucose-concentration dependence that is similar to that of native pancreatic islets (37, 38). As illustrated in Figure 9, insulin secretion from the 832/13 INS-1 cells in response to glucose increases in a concentration-dependent manner between 0 and 20 mM. At 20 mM glucose, the increase in insulin secretion is nearly 8-fold over basal levels. The cyclic AMP (cAMP)-elevating agents forskolin (FSK) (Figure 9) and IBMX (data not shown) amplify glucose-induced secretion to 20–25-fold over basal levels, as in native islets (35, 39). Following treatment of 832/13 INS-1 cells with BEL, insulin secretion in response to glucose without and with forskolin is reduced to near basal levels (Figure 9), suggesting that a BEL-sensitive target such as $iPLA_2\beta$ participates in stimulated insulin secretion from 832/13 INS-1 cells.

Islet $iPLA_2\beta$ Protein and Message

The previously described findings suggest that the predominantly expressed $iPLA_2\beta$ in the INS-1 insulinoma cells is a 70 kDa isoform, that it is catalytically active, and that its

inhibition with BEL does not affect phospholipid remodeling but leads to suppressed glucose-stimulated insulin secretion in 832/13 INS-1 cells. If the shorter isoform of iPLA$_2$β has a role in signal transduction in β-cells, it might be expected to be evident in native islets as well. Immunoblotting analyses confirm that pancreatic islets, in fact, also predominantly express the 70 kDa iPLA$_2$β-immunoreactive protein (Figure 10A). To determine whether the pancreatic islet and 832/13 INS-1 cell enzymes arise from different iPLA$_2$β transcripts, the message expressed in each was compared. As seen in Figure 10B, the 832/13 INS-1 cell sequence deduced from PCR analyses using overlapping primer sets is identical to the iPLA$_2$β message encoding an 84 kDa full-length iPLA$_2$β protein expressed in pancreatic islets (7), suggesting a common origin for the 70 kDa iPLA$_2$β-immunoreactive protein expressed in native islets and 832/13 INS-1 cells. The finding of a 70 kDa isoform of iPLA$_2$β in pancreatic islets also indicates that its expression is not unique to engineered insulinoma cells and raises the possibility that it serves a functionally important role in native β-cells.

DISCUSSION

Approaches to treating insulin-dependent diabetes mellitus include transplantation of whole pancreas or isolated pancreatic islets, but the paucity of the human donor pool has prompted investigators to explore the feasibility of using transplantable insulinoma cells in diabetes therapy (40–44). Attempts to engineer insulinoma cells with increased and stable glucose-stimulated insulin secretory capacity have resulted in the generation of a robustly glucose-responsive 832/13 INS-1 cell line (38).

A difficulty in engineering a stable glucose-responsive cell line is that the glucose sensing mechanism within the β-cell is not completely understood. Pancreatic islets, β-cells, and glucose-responsive insulinoma cells all express a Ca^{2+}-independent PLA$_2$ (iPLA$_2$β) that is stimulated by ATP and is BEL-sensitive (6, 7, 33–36). Inhibition of iPLA$_2$β activity with BEL leads to suppression (6, 7, 33–36) and overexpression of iPLA$_2$β to amplification (5, 28) of glucose-stimulated insulin secretion. The iPLA$_2$β, like cPLA$_2$ (45, 46), translocates to the perinuclear region of β-cells following stimulation, and this involves cAMP-dependent PKA-catalyzed phosphorylation events (28). These and other (5, 31, 47, 48) findings suggest that iPLA$_2$β is involved in signal transduction, but not in phospholipid remodeling, in β-cells.

The findings that iPLA$_2$β amplifies glucose-stimulated insulin secretion as well as β-cell proliferation (49) raises the possibility that β-cells engineered to overexpress iPLA$_2$β might have a place in diabetes therapy. A motive for the present study was to determine whether iPLA$_2$β has a similar signaling role in the robustly glucose-responsive 832/13 INS-1 cells. If so, inclusion of the iPLA$_2$β gene into the iterative engineering process (38, 43, 50–53) to optimize secretory capacity in a transplantable and replenishable source of insulinoma cells might deserve consideration.

An unexpected finding in the present study was that the predominant iPLA$_2$β-immunoreactive protein in the 832/13 INS-cells and in the parental INS-1 cell line migrates with an apparent molecular mass of ca. 70 kDa on SDS-PAGE analyses. While two alternatively spliced iPLA$_2$β cDNA variants have been cloned, which encode proteins with masses of 84 and 88 kDa (20, 21), the 70 kDa protein expressed in unstimulated cells potentially represents a previously unrecognized isoform of iPLA$_2$β.

A mechanism for generation of a short isoform of iPLA$_2$β might involve alternate splicing of iPLA$_2$β transcript. One alternatively spliced mRNA species for iPLA$_2$β in human B-lymphocytes encodes a protein with a molecular mass of 88 kDa (21). This mRNA species

contains a sequence encoded by an exon that is not included in the mRNA species that encode the 84 kDa iPLA$_2$β isoform that was first cloned from rodent sources (7, 19). The 88 kDa iPLA$_2$β isoform contains a 54-amino acid residue insert in the eighth ankyrin repeat (20, 21) that is absent from the 84 kDa iPLA$_2$β isoform. In addition to the full-length iPLA$_2$β, three other iPLA$_2$β mRNA species have been reported to be produced by alternate splicing (21, 22). One encodes a protein that terminates after the lipase active site, and the other two encode proteins that contain only the ankyrin repeats and are inactive (21). Transcripts encoding functionally distinguishable short (84 kDa) and long (88 kDa) forms of iPLA$_2$β have also been observed in human lymphocytes and in pancreatic islets and arise from an exon-skipping mechanism of alternate splicing (20, 21). These observations raise the possibility that alternate splicing might represent a means to generate various iPLA$_2$β isoforms with different functions in different cells. However, examination of this possibility in the present study using overlapping primer sets to amplify the iPLA$_2$β message reveal that the 832/13 INS-1 cell express an iPLA$_2$β message identical to the one expressed in native islets (7) that encodes a full-length 84 kDa iPLA$_2$β protein. These findings suggest that the 70 kDa iPLA$_2$β-immunoreactive protein does not arise from an exon-skipping mechanism of alternate splicing but most likely is a product of, as yet undetermined, a proteolytic processing mechanism.

Whether the short immunoreactive band observed in INS-1 cells is an isoform of iPLA$_2$β was addressed using mass spectrometry to analyze tryptic digests from the 70 kDa region containing iPLA$_2$β-immunoreactive protein. MALDI/TOF/MS analyses reveal at least 10 peptides with m/z values expected of tryptic peptides from iPLA$_2$β. Tandem analyses were then performed to determine the amino acid sequences of these peptides.

Analyses of tandem spectrum obtained from each peptide using the MassLynx software identified several peptides (Table 1) with amino acid sequences that exactly matched fragments expected from digestion of the iPLA$_2$β protein with trypsin. Features of interest include the fact that among the identified peptides were three sequences (6, 9, and 10) encompassing iPLA$_2$β residues 7–53. In addition, the peptide nearest the C-terminus of the iPLA$_2$β deduced sequence ended at residue 555. These findings suggest that the iPLA$_2$β-immunoreactive protein migrating with an apparent molecular mass of 70 kDa is indeed an iPLA$_2$β isoform that contains a conserved N-terminus region and that might lack a C-terminal protein sequence beyond amino acid residue 555.

In view of the inability to visualize an iPLA$_2$β-immunoreactive protein with a molecular mass of 84–88 kDa in the 832/13 INS-1 cells, it was of interest to determine if a iPLA$_2$β enzymatic activity is indeed expressed in these cells. We report here that the 832/13 INS-1 cells express a iPLA$_2$ activity that is stimulated by ATP and is inhibited by BEL. These are properties expected of iPLA$_2$β and are also associated with iPLA$_2$β expressed in pancreatic islets (6, 33, 34), suggesting that the iPLA$_2$β catalytic activity expressed in the 832/13 INS-1 cells is most likely attributable to an isoform of the protein with an apparent molecular mass of 70 kDa.

As a truncated isoform of iPLA$_2$β appears to be responsible for the enzymatic activity in 832/13 INS-1, the question of whether it participates in phospholipid remodeling or signal transduction was addressed. Supplementation of culture medium with arachidonic acid led to the remodeling of 832/13 INS-1 cell membrane phospholipids, as reflected by an increased incorporation of arachidonic acid into PC pools, and this was not inhibited by BEL. However, glucose-induced and forskolin-amplified insulin secretion were significantly suppressed by BEL. These findings suggest that the iPLA$_2$β activity expressed in 832/13 INS-1 cells participates in signal transduction in insulin secretion but not in phospholipid remodeling.

Our present findings therefore demonstrate that a 70 kDa iPLA$_2$β-immunoreactive protein expressed in 832/13 INS-1 cells is indeed a previously unrecognized iPLA$_2$β isoform. They also suggest that this short iPLA$_2$β isoform is catalytically active, BEL-sensitive, and involved in glucose-stimulated insulin secretion. In view of the report demonstrating tissue-specific expression of different iPLA$_2$β isoforms (22), it might be speculated that expression of the 70 kDa iPLA$_2$β isoform is unique to engineered insulinoma cells. However, immunoblotting analyses reveal a similar predominant expression of a 70 kDa iPLA$_2$β-immunoreactive protein in pancreatic islets, although the native islets also express a message, identical to the iPLA$_2$β transcript expressed in the 832/13 INS-1 cells, that encodes a full-length 84 kDa iPLA$_2$β protein (7). These findings raise the possibility that the 70 kDa isoform of iPLA$_2$β serves a functionally important role in signal transduction in the native β-cell.

Acknowledgments

The authors would like to thank Mr. Alan Bohrer, Dr. Mary Wohltmann, Dr. Chun Jin, and Ms. Heather Schmidt for their expert technical assistance.

REFERENCES

1. Gijon MA, Leslie CC. Phospholipases A$_2$. Cell Dev. Biol. 1997; s8:297–303.
2. Dennis EA. The growing phospholipase A$_2$ superfamily of signal transduction enzymes. Trends Biochem. Sci. 1997; 22:1–2. [PubMed: 9020581]
3. Mancuso DJ, Jenkins CM, Gross RW. The genomic organization, complete mRNA sequence, cloning, and expression of a novel human intracellular membrane-associated calcium-independent phospholipase A$_2$. J. Biol. Chem. 2000; 275:9937–9945. [PubMed: 10744668]
4. Tanaka H, Takeya R, Sumimoto H. A novel intracellular membrane-bound calcium-independent phospholipase A$_2$. Biochem. Biophys. Res. Commun. 2000; 272:320–326. [PubMed: 10833412]
5. Ma Z, Ramanadham S, Bohrer A, Wohltmann M, Zhang S, Turk J. Studies of insulin secretory responses and of arachidonic acid incorporation into phospholipids of stably transfected insulinoma cells that overexpress group VIA phospholipase A$_2$ (iPLA$_2$β) indicate a signaling rather than a housekeeping role for iPLA$_2$β. J. Biol. Chem. 2001; 276:13198–13208. [PubMed: 11278673]
6. Gross RW, Ramanadham S, Kruszka KK, Han X, Turk J. Rat and human pancreatic islet cells contain a calcium ion independent phospholipase A$_2$ activity selective for hydrolysis of arachidonate, which is stimulated by adenosine triphosphate and is specifically localized to islet β-cells. Biochemistry. 1993; 32:327–336. [PubMed: 8418853]
7. Ma Z, Ramanadham S, Kempe K, Chi XS, Ladenson JL, Turk J. Pancreatic islets express a Ca^{2+}-independent phospholipase A$_2$ enzyme that contains a repeated structural motif homologous to the integral membrane protein binding domain of ankyrin. J. Biol. Chem. 1997; 272:11118–11127. [PubMed: 9111008]
8. Balsinde SE, Bianco ID, Ackerman EJ, Conde-Frieboes K, Dennis EA. Inhibition of calcium-independent phospholipase A$_2$ prevents arachidonic acid incorporation and phospholipid remodeling in P388D1 macrophages. Proc. Natl. Acad. Sci. 1995; 92:8527–8531. [PubMed: 7667324]
9. Balsinde J, Balboa MA, Dennis EA. Antisense inhibition of group VI Ca^{2+}-independent phospholipase A$_2$ blocks phospholipid fatty acid remodeling in murine P388D1 macrophages. J. Biol. Chem. 1977; 272:29317–29321. [PubMed: 9361012]
10. Chilton FH, Fonteh AN, Suarette ME, Triggiani M, Winkler JD. Control of arachidonate levels within inflammatory cells. Biochim. Biophys. Acta. 1996; 1299:1–15. [PubMed: 8555241]
11. Dennis EA. The biosynthesis of phospholipids. Methods Enzymol. 1992; 209:1–4. [PubMed: 1495408]
12. Williams SD, Ford DA. Calcium-independent phospholipase A$_2$ mediates CREB phosphorylation and *c*-fos expression during ischemia. Am. J. Physiol. 2001; 281:H168–H176.

13. Maggi LB Jr. Moran JM, Scarim AL, Ford DA, Yoon JW, McHowat J, Buller RM, Corbett JA. Novel role for calcium-independent phospholipase A_2 in the macrophage antiviral response of inducible nitric-oxide synthase expression. J. Biol. Chem. 2002; 277:38449–38455. [PubMed: 12167650]
14. Isenovic E, LaPointe MC. Role of Ca^{2+}-independent phospholipase A_2 in the regulation of inducible nitric oxide synthase in cardiac myocytes. Hypertension. 2000; 35:249–254. [PubMed: 10642306]
15. Tithof PK, Peters-Golden M, Ganey PE. Distinct phospholipases A_2 regulate the release of arachidonic acid for eicosanoid production and superoxide anion generation in neutrophils. J. Immunol. 1998; 160:953–960. [PubMed: 9551934]
16. Tithof PK, Olivero J, Ruehle K, Ganey PE. Activation of neutrophil calcium-dependent and -independent phospholipases A_2 by organochlorine compounds. Toxicol. Sci. 2000; 53:40–47. [PubMed: 10653519]
17. Derrickson BH, Mandel LJ. Parathyroid hormone inhibits Na^+-K^+-ATPase through Gq/G11 and the calcium-independent phospholipase A_2. Am. J. Physiol. 1007; 272:F781–F788. [PubMed: 9227640]
18. Boilard E, Surette ME. Anti-CD3 and concanavalin A-induced human T cell proliferation is associated with an increased rate of arachidonate-phospholipid remodeling. Lack of involvement of group IV and group VI phospholipase A_2 in remodeling and increased susceptibility of proliferating T cells to CoA-independent transacyclase inhibitor-induced apoptosis. J. Biol. Chem. 2001; 276:17568–17575. [PubMed: 11278296]
19. Tang J, Kriz RW, Wolfman N, Shaffer M, Seehra S, Jones S. A novel cytosolic calcium-independent phospholipase A_2 contains eight ankyrin motifs. J. Biol. Chem. 1997; 272:8567–8575. [PubMed: 9079687]
20. Ma Z, Wang X, Nowatzke W, Ramanadham S, Turk J. Human pancreatic islets express mRNA species encoding two distinct catalytically active isoforms of group VI phospholipase A_2 ($iPLA_2$) that arise from an exon-skipping mechanism of alternative splicing of the transcript from the $iPLA_2$ gene on chromosome 22q13.1. J. Biol. Chem. 1999; 274:9607–9616. [PubMed: 10092647]
21. Larsson PK, Claesson H-E, Kennedy BP. Multiple splice variants of the human calcium-independent phospholipase A_2 and their effect on enzyme activity. J. Biol. Chem. 1998; 273:207–214. [PubMed: 9417066]
22. Larsson Forsell PK, Kennedy BP, Claesson H-E. The human calcium-dependent phospholipase A_2 gene. Multiple enzymes with distinct properties from a single gene. Eur. J. Biochem. 1999; 262:575–585. [PubMed: 10336645]
23. Atsumi G, Murakami M, Kojima K, Hadano A, Tajima M, Kudo I. Distinct roles of two intracellular phospholipase A_2s in fatty acid release in the cell death pathway. Proteolytic fragment of type IVA cytosolic phospholipase $A_2\alpha$ inhibits stimulus-induced arachidonate release, whereas that of type VI Ca^{2+}-independent phospholipase A_2 augments spontaneous fatty acid release. J. Biol. Chem. 2000; 275:18248–18258. [PubMed: 10747887]
24. Jenkins CM, Wolf MJ, Mancuso DJ, Gross RW. Identification of the calmodulin-binding domain of recombinant calcium-independent phospholipase $A_2\beta$. Implications for structure and function. J. Biol. Chem. 2001; 276:7129–7135. [PubMed: 11118454]
25. Coffin, JM.; Varmus, HE. Retrovirus. Cold Spring Harbor Laboratory Press; Woodbury, NY: 1996.
26. Ramanadham S, Hsu F-F, Zhang S, Bohrer A, Ma Z, Turk J. Electrospray ionization mass spectrometric analyses of phospholipids from INS-1 insulinoma cells: Comparison to pancreatic islets and effects of fatty acid supplementation on phospholipid composition and insulin secretion. Biochim. Biophys. Acta. 2000; 1484:251–266. [PubMed: 10760474]
27. Mulder H, Lu D, Finley J IV, An J, Cohen J, Antinozzi PA, McGarry JD, Newgard CB. Overexpression of a modified human malonyl-CoA decarboxylase blocks the glucose-induced increase in malonyl-CoA level but has no impact on insulin secretion in INS-1-derived (832/13) α-cells. J. Biol. Chem. 2001; 276:6479–6484. [PubMed: 11113153]
28. Ma Z, Zhang S, Turk J, Ramanadham S. Stimulation of insulin secretion and associated nuclear accumulation of $iPLA_2\alpha$ in INS-1 insulinoma cell. Am. J. Physiol. Endocrinol. Metab. 2002; 282:E820–E833. [PubMed: 11882502]

29. Ramanadham S, Zhang S, Ma Z, Wohltmann M, Bohrer A, Hsu F-F, Turk J. Delta 6-, stearoyl CoA-, and delta 5-desaturase enzymes are expressed in α-cells and are altered by increases in exogenous PUFA concentrations. Biochim. Biophys. Acta. 2002; 1580:40–56. [PubMed: 11923099]
30. Ramanadham S, Wolf MJ, Jett PA, Gross RW, Turk J. Characterization of an ATP-stimulatable Ca^{2+}-independent phospholipase A_2 from clonal insulin-secreting HIT cells and rat pancreatic islets: A possible molecular component of the α-cell fuel sensor. Biochemistry. 1994; 32:7442–7452. [PubMed: 8003509]
31. Ramanadham S, Hsu F-F, Bohrer A, Ma Z, Turk J. Studies of the role of group VI phospholipase A_2 in fatty acid incorporation, phospholipid remodeling, lysophosphatidylcholine generation, and secretagogue-induced arachidonic acid release in pancreatic islets and insulinoma cells. J. Biol. Chem. 1999; 274:13915–13927. [PubMed: 10318801]
32. Hsu F-F, Bohrer A, Turk J. Formation of lithiated adducts of glycerophosphocholine lipids facilitates their identification by electrospray ionization tandem mass spectrometry. J. Am. Soc. Mass Spectrom. 1998; 9:516–526. [PubMed: 9879366]
33. Ma Z, Ramanadham S, Hu Z, Turk J. Cloning and expression of a group IV cytosolic Ca^{2+}-dependent phospholipase A_2 from rat pancreatic islets. Comparison of the expressed activity with that of an islet group VI cytosolic Ca^{2+}-independent phospholipase A_2. Biochim. Biophys. Acta. 1998; 1391:384–400. [PubMed: 9555100]
34. Ramanadham S, Wolf M, Li B, Bohrer A, Turk J. Glucose-responsitivity and expression of an ATP-stimulatable, Ca^{2+}-independent phospholipase A_2 enzyme in clonal insulinoma cell lines. Biochim. Biophys. Acta. 1997; 1344:153–164. [PubMed: 9030192]
35. Ramanadham S, Gross RW, Han X, Turk J. Inhibition of arachidonate release by secretagogue-stimulated pancreatic islets suppresses both insulin secretion and the rise in α-cell cytosolic calcium ion concentration. Biochemistry. 1993; 32:337–346. [PubMed: 8418854]
36. Ma Z, Turk J. The molecular biology of the group VIA Ca^{2+}-independent phospholipase A_2. Prog. Nucleic Acid Res. Mol. Biol. 2001; 67:1–33. [PubMed: 11525380]
37. Zawalich WS, Zawalich KC. Regulation of insulin secretion by phospholipase C. Am. J. Physiol. 1996; 271:E409–E416. [PubMed: 8843732]
38. Hohmeier HE, Mulder H, Chen G, Henkel-Rieger R, Prentki M, Newgard CB. Isolation of INS-1-derived cell lines with robust ATP-sensitive K^+ channel-dependent and -independent glucose-stimulated insulin secretion. Diabetes. 2000; 49:424–430. [PubMed: 10868964]
39. Turk J, Gross R, Ramanadham S. Amplification of insulin secretion by lipid messengers. Diabetes. 1993; 42:367–374. [PubMed: 8432406]
40. Poitout V, Olson LK, Robertson RP. Insulin-secreting cell lines: Classification, characteristics, and potential applications. Diabetes Metab. 1996; 22:7–14. [PubMed: 8697299]
41. Newgard CB, Clark S, Beltrandel-Rio H, Hohmeier HE, Quaade C, Normington K. Engineered cell lines for insulin replacement in diabetes: Current status and future prospects. Diabetologia. 1997; 40:S42–S47. [PubMed: 9248700]
42. Chen G, Hohmeier HE, Gasa R, Tran VV, Newgard CB. Selection of insulinoma cell lines with resistance to interleukin-1 B- and γ-interferon-induced cytotoxicity. Diabetes. 2000; 49:562–570. [PubMed: 10871193]
43. Xu R, Li H, Tse LY, Kung HF, Lu H, Lam KS. Diabetes gene therapy: Potential and challenges. Curr. Gene Ther. 2003; 3:65–82. [PubMed: 12553537]
44. Asfari M, Janjic D, Meda P, Li G, Halban PA, Wollheim CB. Establishment of 2-mercaptoethanol-dependent differentiated insulin-secreting cell lines. Endocrinology. 1992; 130:167–178. [PubMed: 1370150]
45. de Carvalho MG, McCormack AL, Olson E, Ghomashchi F, Gelb MH, Yates JR III, Leslie CC. Identification of phosphorylation sites of human 85 kDa cytosolic phospholipase A_2 expressed in insect cells and present in human monocytes. J. Biol. Chem. 1996; 271:6987–6997. [PubMed: 8636128]
46. Glover S, de Carvalho MS, Bayburt T, Jonas M, Chi E, Leslie CC, Gelb MH. Translocation of the 85 kDa phospholipase A_2 from cytosol to the nuclear envelope in rat basophilic leukemia cells

stimulated with calcium ionophore or IgE/antigen. J. Biol. Chem. 1995; 270:15359–15367. [PubMed: 7797525]

47. Owada S, Larsson O, Arkhammar P, Katz AI, Chibalin AV, Berggren PO, Bertorello AM. Glucose decreases Na^+, K^+-ATPase activity in pancreatic β-cells. An effect mediated via Ca^{2+}-independent phospholipase A_2 and protein kinase C-dependent phosphorylation of the α-subunit. J. Biol. Chem. 1999; 274:2000–2008. [PubMed: 9890957]
48. Simonsson E, Karlsson S, Ahren B. Ca^{2+}- independent phospholipase A_2 contributes to the insulinotropic action of cholecystokinin-8 in rat islets: Dissociation from the mechanism of carbachol. Diabetes. 1998; 47:1436–1443. [PubMed: 9726232]
49. Ma Z, Bohrer A, Wohltmann M, Ramanadham S, Hsu F-F, Turk J. Studies of phospholipid metabolism, proliferation, and secretion of stably transfected insulinoma cells that overexpress group VIA phospholipase A_2. Lipids. 2001; 36:689–700. [PubMed: 11521967]
50. Simonsson E, Ahren B. Phospholipase A_2 and its potential regulation of islet function. Int. J. Pancreatol. 2000; 27:1–11. [PubMed: 10811018]
51. Clark SA, Quaade C, Constandy H, Hansen P, Halban P, Ferber S, Newgard CB, Normington K. Novel insulinoma cell lines produced by iterative engineering of GLUT2, glucokinase, and human insulin expression. Diabetes. 1997; 46:958–967. [PubMed: 9166666]
52. Noel RJ, Antinozzi PA, McGarry JD, Newgard CB. Engineering of glycerol-stimulated insulin secretion in islet β-cells. Differential metabolic fates of glucose and glycerol provide insight into mechanisms of stimulus-secretion coupling. J. Biol. Chem. 1997; 272:18621–18627. [PubMed: 9228030]
53. Chen G, Hohmeier HE, Newgard CB. Expression of the transcription factor STAT-1 α in insulinoma cells protects against cytotoxic effects of multiple cytokines. J. Biol. Chem. 2001; 276:766–772. [PubMed: 11024034]

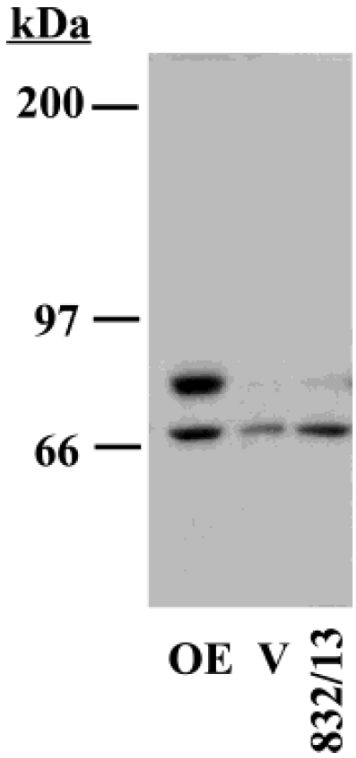

Figure 1.
Immunoblotting analyses of iPLA$_2$β-immunoreactive protein expression in 832/13 INS-1 cells. Aliquots (50 μg) of cytosol prepared from INS-1 cells transfected with either an empty vector (V) or vector containing iPLA$_2$β cDNA construct (OE) and from 832/13 INS-1 cells were analyzed by SDS–PAGE, and the proteins were transferred onto immobolin-P PVDF membrane. The electroblot was then processed for immunoblotting analyses, and immunoreactive iPLA$_2$β protein was visualized by ECL.

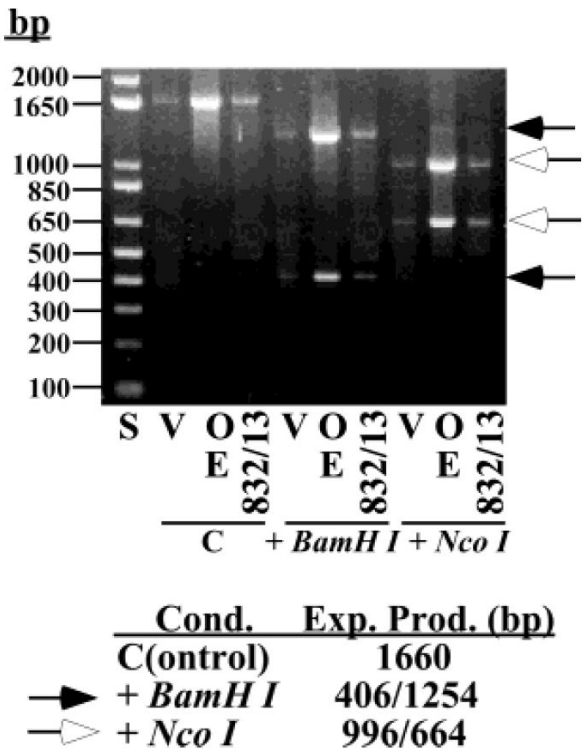

Figure 2.

Expression of $iPLA_2\alpha$ message in 832/12 INS-1 cells. Following total RNA isolation from INS-1 cells transfected with either an empty vector (V) or a vector containing the $iPLA_2\beta$ cDNA construct (OE) and from 832/13 INS-1 cells, cDNA was prepared from 6 μg of RNA by RT reaction. PCR analyses for $iPLA_2\beta$ were then performed using the primer set described in the Materials and Methods. The first three lanes of samples represent undigested PCR products, and the second (*Bam H I*) and third (*Nco I*) set of lanes represent restriction enzyme digested PCR products. The PCR products were analyzed on 1.0% agarose gels and visualized by ethidium bromide staining. (S denotes a standard mixture of cDNA species of known length expressed in base pairs.)

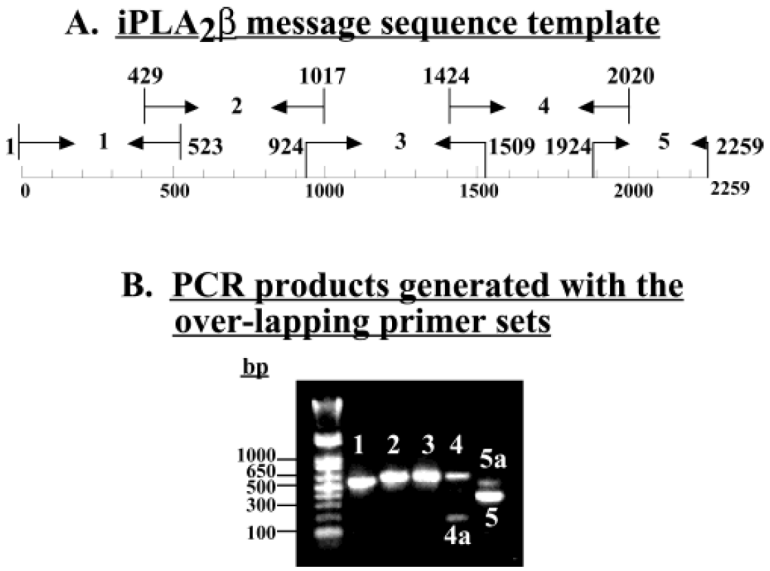

Figure 3.

Expression of the full-length iPLA$_2\alpha$ message in 832/12 INS-1 cells. Following total RNA isolation from 832/13 INS-1 cells, cDNA was prepared from 6 μg of RNA by RT reaction. PCR analyses were then performed for iPLA$_2\alpha$ using five overlapping primer sets (1–5), described in the Materials and Methods. (A) Template of the iPLA$_2\beta$ message sequence and the regions targeted for amplification by the five primer sets. (B) PCR was performed in the presence of each primer set separately, and the resulting reaction products were analyzed on 1.0% agarose gels and visualized by ethidium bromide staining. The expected product size (bp) with each primer set is as follows: (1) 523, (2) 589, (3) 586, (4) 597, and (5) 336. The PCR bands 4a and 5a were nonspecific products whose sequences had no homology with the iPLA$_2\beta$ mRNA sequence.

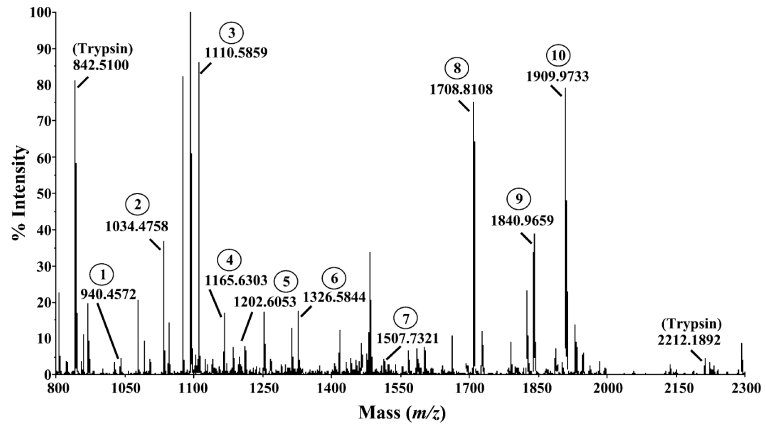

Figure 4.

MALDI/TOF/MS spectrum of tryptic digest of from iPLA$_2$β immunoreactive protein in the 70 kDa region of SDS–PAGE gels. An aliquot of the tryptic digest of the 70 kDa protein illustrated in Figure 1 was mixed with α-cyano-4-hydroxycinnamic acid matrix and spotted onto a MALDI plate prior to MS analyses. The numbered $[M + H]^+$ ions (1–10) exhibit *m*/*z* values expected of tryptic peptides from iPLA$_2$β protein.

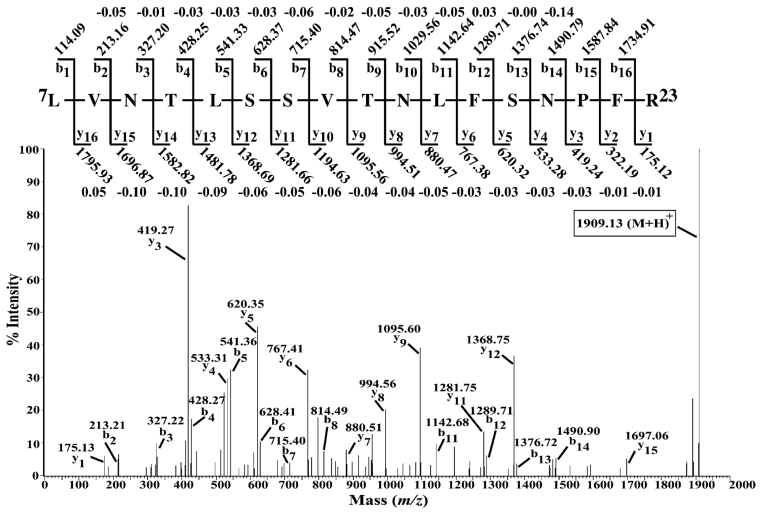

Figure 5.

Tandem spectrum of the $[M + H]^{+2}$ ion at *m/z* 955.03 of tryptic peptides from a 70 kDa iPLA$_2$β digest. An aliquot of the tryptic digest analyzed by MALDI/TOF/MS, illustrated in Figure 4, was analyzed by LC/ESI/MS, and the $[M + H]^{+2}$ ion at *m/z* 955.03 was analyzed by tandem MS. The observed tandem spectra of the $[M + H]^{+2}$ ion at *m/z* 955.03 produced by CAD is displayed and include the *y*- and *b*-series ions expected from the peptide sequence, illustrated in the inset. Inset: The expected peptide fragmentation patterns of the candidate peptide LVNTLSSVTNLFSNPFR with the $[M + H]^{+2}$ *m/z* of 955.03. The expected masses of *b*- and *y*-series ions and their deviation from observed masses are listed, respectively, above and below the expected *m/z* values.

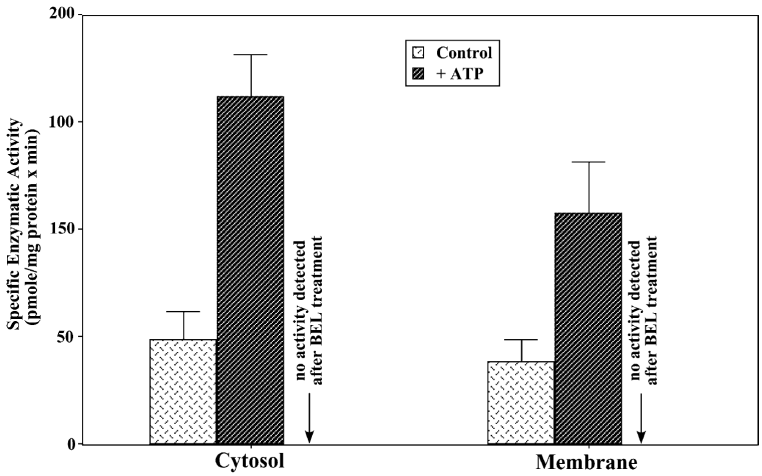

Figure 6.

ATP stimulation and BEL inhibition of iPLA$_2$β enzymatic activity in 832/13 INS-1 cells. Cytosolic and membrane fractions were prepared from 832/13 INS-1 cells, and Ca^{2+}-independent PLA$_2$ (iPLA$_2$β) activity was assayed in aliquots of protein (30 μg) incubated (37 °C, 5 min) in the presence of EGTA (5 mM) with substrate [^{14}C]-PLPC. Subsequently, hydrolyzed [^{14}C]-linoleate was quantified by liquid scintillation spectrometry, and the calculated specific enzymatic activity is displayed. The data are expressed as means ± SEM (n = 6–10) of specific iPLA$_2$β enzymatic activity (pmol/mg of protein × min).

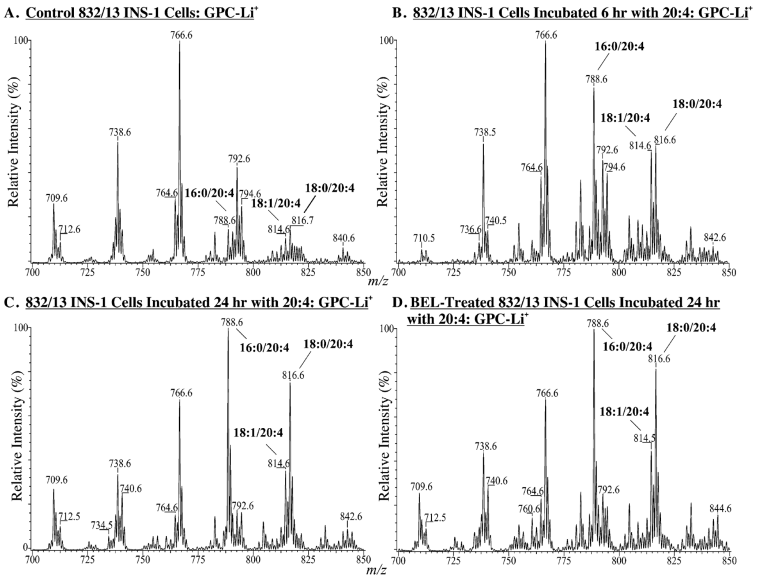

Figure 7.

ESI/MS analyses of glycerophosphocholine (GPC) lipid species in 832/13 INS-1 cells supplemented with arachidonic acid in the absence or presence of BEL. 832/13-INS-1 cells were treated with either vehicle alone (A), with arachidonic acid for 6 h (B) or 24 h (C), or pretreated with BEL (25 μM) prior to arachidonic acid supplementation for 24 h (D). Lipids were extracted and analyzed as Li^+ adducts by ESI/MS/MS in positive ion mode by scanning for precursor ions that undergo neutral loss of 183. This loss reflects the elimination of phosphocholine headgroup and identifies GPC lipids (18, 36).

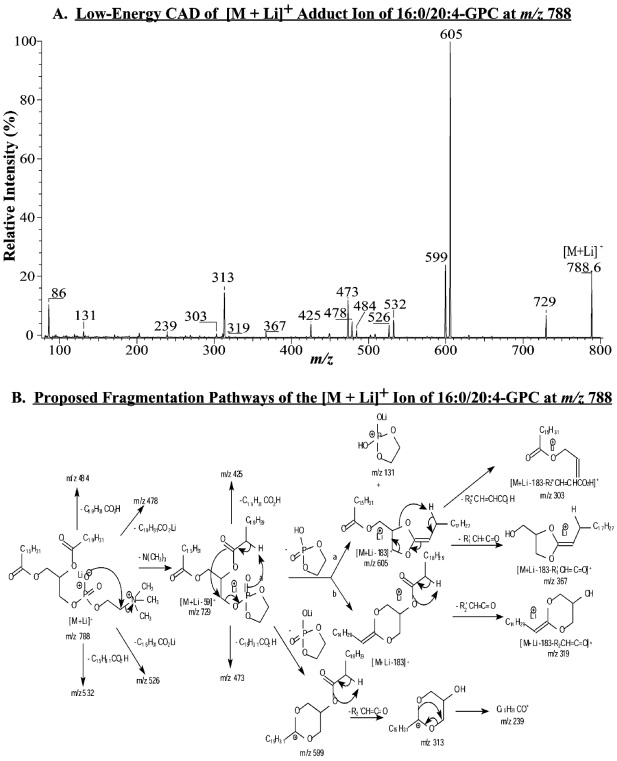

Figure 8.

Tandem mass spectra obtained from collisionally-activated dissociation (CAD) of $[M + Li]^+$ ions of GPC lipids from 832/13 INS-1 cells. ESI/MS was performed as in Figure 7, and the $[M + Li]^+$ ion at *m/z* 788 was isolated in the first quadrupole and subjected to CAD. Product ions were then analyzed in the final quadrupole. (A) CAD $[M + Li]^+$ ion at *m/z* 788. (B) Fragmentation pattern of $[M + Li]^+$ ion at *m/z* 788.

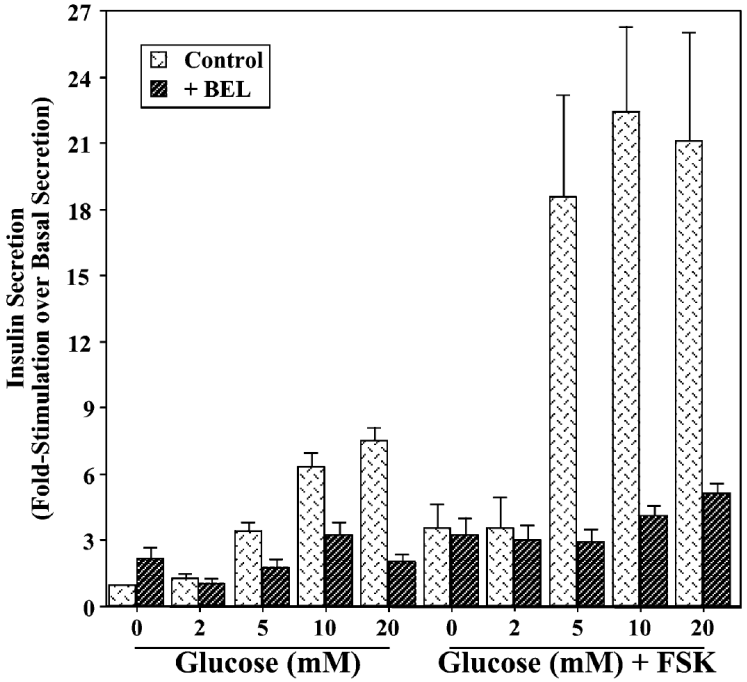

Figure 9.

Insulin secretion from 832/13 INS-1 cells. Cells were seeded in 24-well plates and incubated (1 h, 37 °C, 95% air/5% CO_2) in KRB medium containing glucose alone or glucose plus forskolin (FSK, 2.5 μM) in the absence and presence of BEL (10 μM). At the end of the incubation period, insulin content in the media was determined by RIA. Stimulated increases in insulin secretion are plotted as mean ± SEM, relative to basal (zero glucose) secretion (n = 5–7).

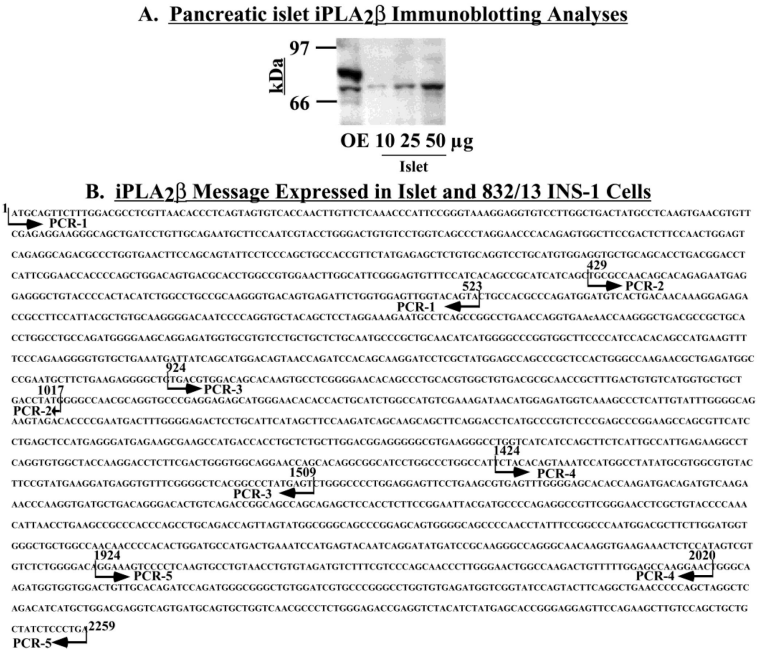

Figure 10.

iPLA$_2$β-immunoreactive protein expression in pancreatic islets and iPLA$_2$β message in islets and 832/13 INS-1 cells. (A) Immunoblotting analyses. Aliquots (10–50 μg) of cytosolic protein prepared from rat pancreatic islets were analyzed by SDS–PAGE, and the proteins were transferred onto immobolin-P PVDF membrane. The electroblot was then processed for immunoblotting analyses, and iPLA$_2$β-immunoreactive protein was visualized by ECL. (OE, iPLA$_2$β-overexpressing INS-1 cells.) (B) Comparison of iPLA$_2$β message in islets and 832/13 cells. The deduced message sequence of islet iPLA$_2$β (7) is illustrated along with the sequence coverage of the PCR products generated using five overlapping primer sets and the 832/13 INS-1 cell cDNA as template. (PCR1–5, sequences of products generated using primer sets 1–5 described in the Materials and Methods, respectively.)

Table 1

Tryptic Fragments of the 70 kDa-Immunoreactive Protein Identified by LC/ESI/MS/MS as Originating from iPLA$_2$β Protein[a]

ID	obs *mlz*	*z*	M_r (calc)	M_r (exp)	delta	*MC*	iPLA$_2$β peptide sequence
10	955.03	+2	1908.06	1908.01	0.05	0	7-LVNTLSSVTNLFSNPFR-23
6	663.82	+2	1325.62	1325.61	0.01	0	26-EVSLADYASSER-37
9	614.01	+3	1839.02	1839.00	0.02	1	38-VREEGQLILLQNQSNR-53
7	503.25	+3	1506.72	1506.72	0.00	0	347-GEHGNTPLHLAM*SK-360
5	601.82	+2	1201.63	1201.61	0.02	0	396-QLQDLMPVSR-405
4	583.33	+2	1164.64	1164.63	0.01	0	408-KPAFILSSM*R-417
1	470.74	+2	939.46	939.45	0.01	1	490-M*KDEVFR-496
8	570.30	+3	1707.87	1707.85	0.02	0	497-GSRPYESGPLEEFLK-511
3	555.81	+2	1109.61	1109.60	0.01	0	538-QPAE†LHLFR-546
2	517.75	+2	1033.49	1033.48	0.01	0	547-NYDAPEAVR-555

Data were processed by Mascot and MassLynx Softwares, and the peptides listed were found to be identical to tryptic fragments expected from the iPLA$_2$β protein. ID, fragment number assigned based on mass identification by MALDI/TOF/MS (Figure 4); obs *mlz*, observed mass with charge state of *z*; M_r, calculated and expected mass of peptide; delta, mass difference between the calculated and expected values; *MC*, number of cleavage sites missed by trypsin during the in-gel digestion procedure; and the last column lists the peptide sequences that matched amino acid residues in the iPLA$_2$β protein. (M*, oxidized methionine; E†, pyroglutamate; and RE and KD, missed trypsin cleavage sites).

[a]Tryptic digest prepared from the iPLA$_2$β-immunoreactive protein in the 70 kDa protein region was analyzed by LC/ESI/MS/MS, and peptide sequences were obtained following tandem analyses.